

Evolution of Hierarchically-Layered Cu-rich Silicide Nano-Architectures

Ibrahim Saana Amiin, Nilotpal. Kapuria, Temilade Esther Adegoke,
Angelika Holzinger, Hugh Geaney, Micheál D. Scanlon, and Kevin M. Ryan

Cryst. Growth Des., **Just Accepted Manuscript** • DOI: 10.1021/acs.cgd.0c00833 • Publication Date (Web): 14 Sep 2020

Downloaded from pubs.acs.org on September 16, 2020

Just Accepted

“Just Accepted” manuscripts have been peer-reviewed and accepted for publication. They are posted online prior to technical editing, formatting for publication and author proofing. The American Chemical Society provides “Just Accepted” as a service to the research community to expedite the dissemination of scientific material as soon as possible after acceptance. “Just Accepted” manuscripts appear in full in PDF format accompanied by an HTML abstract. “Just Accepted” manuscripts have been fully peer reviewed, but should not be considered the official version of record. They are citable by the Digital Object Identifier (DOI®). “Just Accepted” is an optional service offered to authors. Therefore, the “Just Accepted” Web site may not include all articles that will be published in the journal. After a manuscript is technically edited and formatted, it will be removed from the “Just Accepted” Web site and published as an ASAP article. Note that technical editing may introduce minor changes to the manuscript text and/or graphics which could affect content, and all legal disclaimers and ethical guidelines that apply to the journal pertain. ACS cannot be held responsible for errors or consequences arising from the use of information contained in these “Just Accepted” manuscripts.

Evolution of Hierarchically-Layered Cu-rich Silicide Nano-Architectures

Ibrahim Saana Amiinu, Nilotpal Kapuria, Temilade Esther Adegoke, Angelika Holzinger,

Hugh Geaney, Micheál D. Scanlon, Kevin M Ryan*

Bernal Institute, University of Limerick, Limerick, V94 T9PX, Ireland

Department of Chemical Sciences, University of Limerick, Limerick, V94 T9PX, Ireland

ABSTRACT: A solution based synthesis of well-ordered Cu-rich silicide nano-architectures, consisting of a pair of layered cups and stems (ρ -Cu₁₅Si₄) is demonstrated. The as-grown ρ -Cu₁₅Si₄ typically exhibits distinct interconnected 1D stems, consisting of a stack of nanorods (~300 nm in length), terminated with concave hexagonal 3D cups that evolve through a self-regulated layer-by-layer growth mechanism. Discrete-time *ex situ* experimental observations reveal that the ρ -Cu₁₅Si₄ evolution is driven by interatomic diffusion, initially triggering the formation of binary-phase silicide islands (spheres) followed by the formation of hexagonal discs, stem growth, and lateral elongation in exactly opposite directions. It is further shown that electrochemically pre-grown Cu-crystals can facilitate direct growth of the ρ -Cu₁₅Si₄ in high yield with enhanced substrate coverage.

INTRODUCTION

Transition metal silicides (TMS) have a wide range of applications in applied science arising from their inherent compatibility with Si and electronic properties that are compositionally tunable.¹⁻⁸ Common synthesis routes to TMS typically include the conversion of pre-formed Si structures coated with a desired metal precursor by annealing,^{9,10,11} co-precipitation of precursor metal and Si atoms on

1
2 a discrete substrate,^{12,13} or by direct reaction of Si monomers with a desired metal precursor
3
4 substrate.^{14,15} To date, a variety of TMS with tailored functional properties such as MnSi_{1.7} and CrSi₂
5
6 (thermoelectrics),^{16,17} β -FeSi₂ (optics),¹⁸ Co₂MnSi (magnetics),¹⁹ and low resistivity NiSi₂ or PtSi
7
8 nanowires (NWs) for Schottky barriers and gas-sensing devices have been reported.^{20,21}
9

10
11 Of particular interest are Cu-silicides, which are a promising class of materials with potential
12
13 impact on several technological fronts, including uses as Cu-ion diffusion barriers, passivation layers,
14
15 and lithium-ion battery current collectors.^{14,15,22-26} By far, Cu₃Si and its polymorphs is the phase
16
17 predominantly reported compared to the more attractive Cu-rich phase (Cu₁₅Si₄), and is typically
18
19 synthesised *via* solid-state reactions, for example, by evaporation of Cu or CuO powders on Si wafers
20
21 at high temperatures (650–900 °C) or by Au-catalyst assisted vapour transport mechanism at 960
22
23 °C.²⁷⁻²⁹ These approaches have allowed the formation of asymmetric micro-films, squared, triangular,
24
25 and nanorod shaped particles.²⁷⁻³⁰ Single crystal Cu₃Si with defined growth positions have also been
26
27 synthesised *via* a surface energy-driven mechanism at 650 °C.^{1,28} The growth process relies on
28
29 patterned defects on a Si substrate as nucleation centers and a Ge-catalyst to facilitate the surface
30
31 diffusion process.²⁸ A more recent study of the growth mechanism of free-standing Cu₃Si NWs on a
32
33 multilayered Cu/Ge/SiO₂/Si substrate has identified the formation of isolated silicide islands as active
34
35 sites for the NW growth.^{27,29} Combined theoretical and experimental studies have also shown that a
36
37 first-order phase transition occurs through the formation of intermediate state, which significantly
38
39 induces the creation of new-phase nuclei,³¹ and diffusional coalescence of islands on the crystal
40
41 surface can promote faceting, indicating a layer-by-layer growth mechanism.³² The Cu-rich phase
42
43 (Cu₁₅Si₄) is highly desired as it exhibits enhanced electrical/electronic properties, higher oxidation
44
45 resistance/chemical stability, refined crystal structure, higher melting point (>800 °C), and the ability
46
47 to reduce minority-carrier diffusion lengths, *e.g.* for efficient recombination in solar cells.^{4,9,14,26} Thin
48
49 films of Cu₁₅Si₄ have been achieved using solid Cu/Si elements *via* an arc-melting technique.²⁶ In
50
51
52
53
54
55
56
57
58
59
60

1
2 addition to the mixed formation of Cu_3Si intermediates, the procedure necessitates a further sample
3
4 annealing treatment at 780 °C for up to 120 h.
5

6
7 It has been previously demonstrated that the delivery of Si monomer to a metal precursor
8
9 substrate in high-boiling point organic solvents (HBOS) can effectively induce direct growth of
10
11 single-phase Cu-silicide NWs or axial heterostructured Ni-silicide NWs, thus, offering a new route
12
13 to directly synthesise Cu-rich silicides at a lower temperature (460 °C) compared to a all-solid-state
14
15 reaction procedure.^{14,15} However, the process still depends on either Au-catalyst to drive the
16
17 silicidation process (heterostructures),^{15,30} or the formation of underlying Cu-silicide seeds (as self-
18
19 generated catalyst) to activate growth of the NWs.¹⁴ The latter process is further complicated as the
20
21 latent formation of underlying silicide seeds can preferentially induce growth of pure-phase Si NWs,
22
23 through a vapour-solid-solid mechanism, with limited or no silicide NW formation.¹⁴ Moreover, the
24
25 silicide NW growth is non-uniform with disoriented multipod clusters in a wide morphology
26
27 distribution, making insights into the growth mechanism difficult.^{14,15,27,30}
28
29
30
31

32 Herein, for the first time, we demonstrate an in-plane growth mechanism of well-ordered Cu-
33
34 rich silicide nanostems terminated by a concave morphology (hereafter referred to as cup and stem)
35
36 *via* a simple solution approach. Typically, the as-grown silicide ($\rho\text{-Cu}_{15}\text{Si}_4$) exhibits a pair (ρ) of
37
38 interconnected 1D stems with node-internode-like features (stack of nanorods) and concave
39
40 hexagonal 3D cups that evolves through a self-regulated layer-by-layer growth mechanism. The ρ -
41
42 $\text{Cu}_{15}\text{Si}_4$ was synthesised via two distinct approaches, as detailed in the supporting information. In the
43
44 first case, a previously prepared planar Cu-foil was directly used as the growth substrate, while in the
45
46 second case, a single layer of pyramidal Cu-crystals were electrochemically grown on a Cu-foil
47
48 before being used as the growth substrate. The as-prepared substrates were then each subjected to
49
50 similar silicidation process to reveal the prevailing growth mechanism.^{33,34}
51
52
53
54
55
56
57
58
59
60

RESULTS AND DISCUSSION

Material structure and composition

Figure 1a and **b** show SEM images of the hierarchically grown pair of cup-stem architecture with the stems extending up to ~ 3.20 μm in length and ~ 150 nm in diameter. Interestingly, the stems share the same growth crystal base and elongate in exactly opposite directions with comparable topological features in terms of length, shape, and orientation. **Figure 1c** reveals that the stems consist of a stack of nanorods (~ 300 nm in length) interconnected in a fashion akin to the node-internode features of a bamboo stalk (**Figure S1**). As clearly seen in **Figure 1d**, the stem growth (nanorods stacking) is terminated by the formation of well-defined concave structures (cups). **Figure 1e** further reveals that the proliferation of the cup is facilitated by a diffusion-induced formation/deposition of concentric rings of hexagonal layers, stacked into a stair-like morphology, yielding a cup-like feature with sizes proportional to the number of layers (**Figure S2**). Previous reports have shown that such layered and step-wise growth features may be due to a two-dimensional nucleation process occurring on the spherical crystal surface as more Si flux reacts with diffused Cu atoms from the silicides grains, leading to displaced atomic arrangements promoted by the mechanism of screw dislocation.³²⁻³⁴ The average cup size across the outermost vertices and estimated average depth are ~ 1.21 μm and ~ 450 nm, respectively. The Gaussian-fitted size distribution of the hierarchically grown cups and stems is shown in **Figure 1f** and **g**, respectively, with the detailed dimensions illustrated in **Figure 1h**. Chemical composition analysis by energy dispersive X-ray (EDX) spectrum (**Figure S3**) and elemental mapping (**Figure 2i**) confirm the presence and uniform distribution of both Si and Cu in the stem and cup sections, indicating a uniform silicide structure. A cross-sectional analysis by focused ion beam (FIB) milling was also performed to further examine the $\rho\text{-Cu}_{15}\text{Si}_4$ morphology. As shown in **Figure S4**, the FIB-SEM sectioning shows that the dent is only limited to the cup section with the stems being fully solid structures.

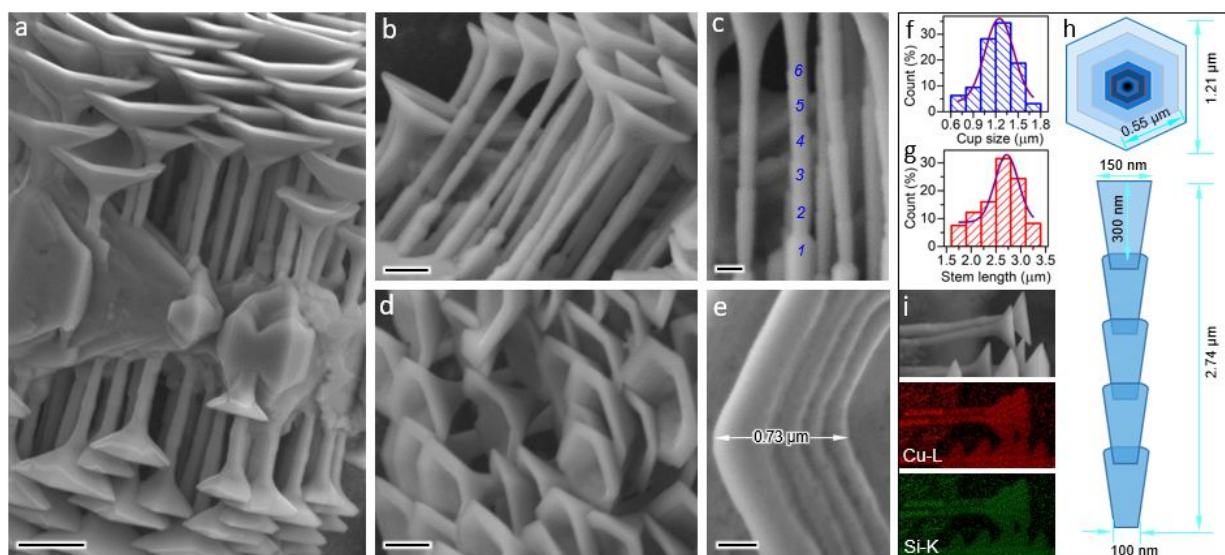


Figure 1 SEM images of the hierarchically grown ρ -Cu₁₅Si₄ architecture. (a) cups and stems feature extending in exactly opposite directions from the same growth crystal base (scale: 1 μ m), (b) selected area of stem-cup section (scale: 0.5 μ m), (c) node-internode features of the stem (scale: 200 nm), numbers indicate the internodes, (d) cups (scale: 0.5 μ m), and (e) stairs-like layered feature of the cup section (scale: 200 nm), and Gaussian-fitted size distribution histogram of (f) cups (average size: $\sim 1.21 \pm 0.5$ μ m) and (g) stems (average size: $\sim 2.74 \pm 0.6$ μ m), (h) Schematic illustration of the grown ρ -Cu₁₅Si₄ geometry showing the mean dimensions, and (i) SEM image and corresponding EDX elemental mapping of Cu (red) and Si (green) distribution in the ρ -Cu₁₅Si₄.

The ρ -Cu₁₅Si₄ crystal structure was further examined in more detail by transmission electron microscopy (TEM) and X-ray diffraction (XRD) analysis. As shown in **Figure 2a-c**, the low resolution TEM images reveal the node-internode features and non-hollow structure of the stems, conforming with the FIB-SEM observations. However, the layered feature of the cup section is not clearly visible due to the high thickness resulting from overlap of the layers. High resolution TEM images (**Figure 2d** and **e**) of the cup section reveals the crystalline structure with high degree of atomic ordering and an interplanar spacing of ~ 2.37 and ~ 2.22 \AA for the (400) and (420) lattice orientations, respectively, as represented in **Figure 2f**. Similar crystalline features are also clearly observed in the stem section (**Figure S5**), indicating that the crystal structure of ρ -Cu₁₅Si₄ is invariant across the cup and stem features. Selected area electron diffraction (SAED) patterns (inset) also show

discrete diffraction spots matching well with that of single crystal $\text{Cu}_{15}\text{Si}_4$ with a high degree of crystallinity.¹⁴

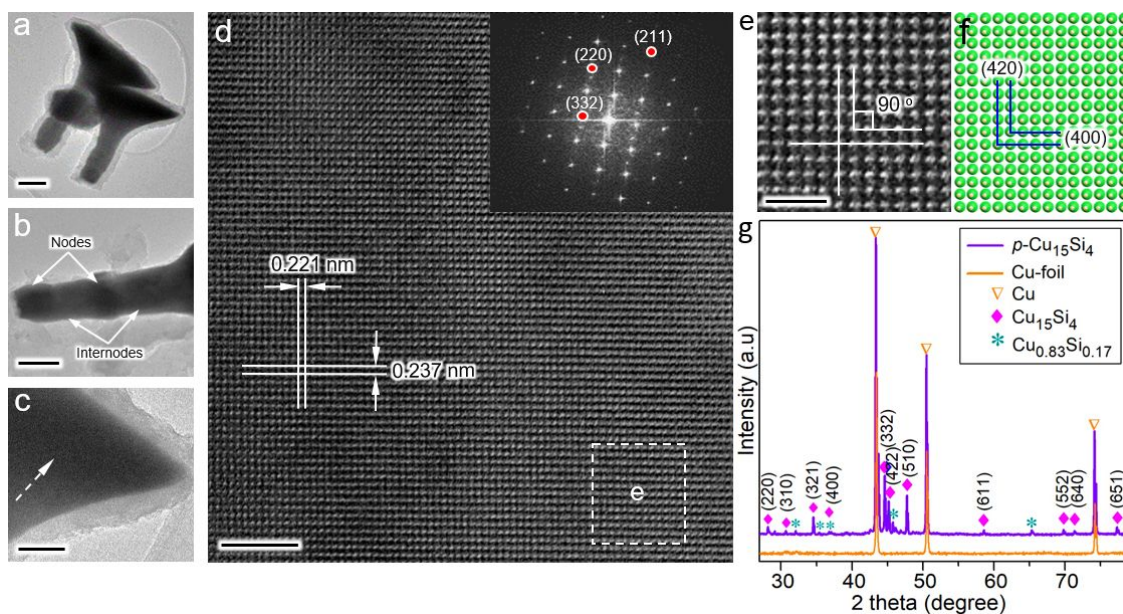


Figure 2 (a) Low resolution TEM image of the $\rho\text{-Cu}_{15}\text{Si}_4$ (scale: 200 nm) and magnified areas along the (b) stem and (c) cup sections (scale: 100 nm), (d) HR-TEM of the cup section (scale: 2 nm) and SAED pattern (inset), (e) Magnified image of the selected area marked by the dashed line in d (scale: 1 nm), and (f) representative model of atomic ordering, (g) X-ray diffraction patterns of $\rho\text{-Cu}_{15}\text{Si}_4$ and the parent Cu-foil.

X-ray diffraction patterns were also collected to verify the crystallinity of the $\rho\text{-Cu}_{15}\text{Si}_4$ structure. As shown in **Figure 2g**, the XRD pattern of $\rho\text{-Cu}_{15}\text{Si}_4$ matches with the diffraction characteristics of a typical $\text{Cu}_{15}\text{Si}_4$ phase (JCPDS: 01-076-1800) with a cubic crystal structure and $\bar{I}4\bar{3}d$ space group.^{14,23,26,35} Minor diffraction peaks assigned to $\text{Cu}_{0.83}\text{Si}_{0.17}$ (JCPDS: 00-023-0223) and intense peaks indexed to the parent Cu-foil (JCPDS: 01-070-3038) are also detected. However, the absence of the $\text{Cu}_{0.83}\text{Si}_{0.17}$ phase from the TEM analysis suggests that it only exists in a preformed silicide layer on the Cu-foil surface prior to the $\rho\text{-Cu}_{15}\text{Si}_4$ growth, conforming with the theory of intermediate state formation via a first-order phase transition.³²

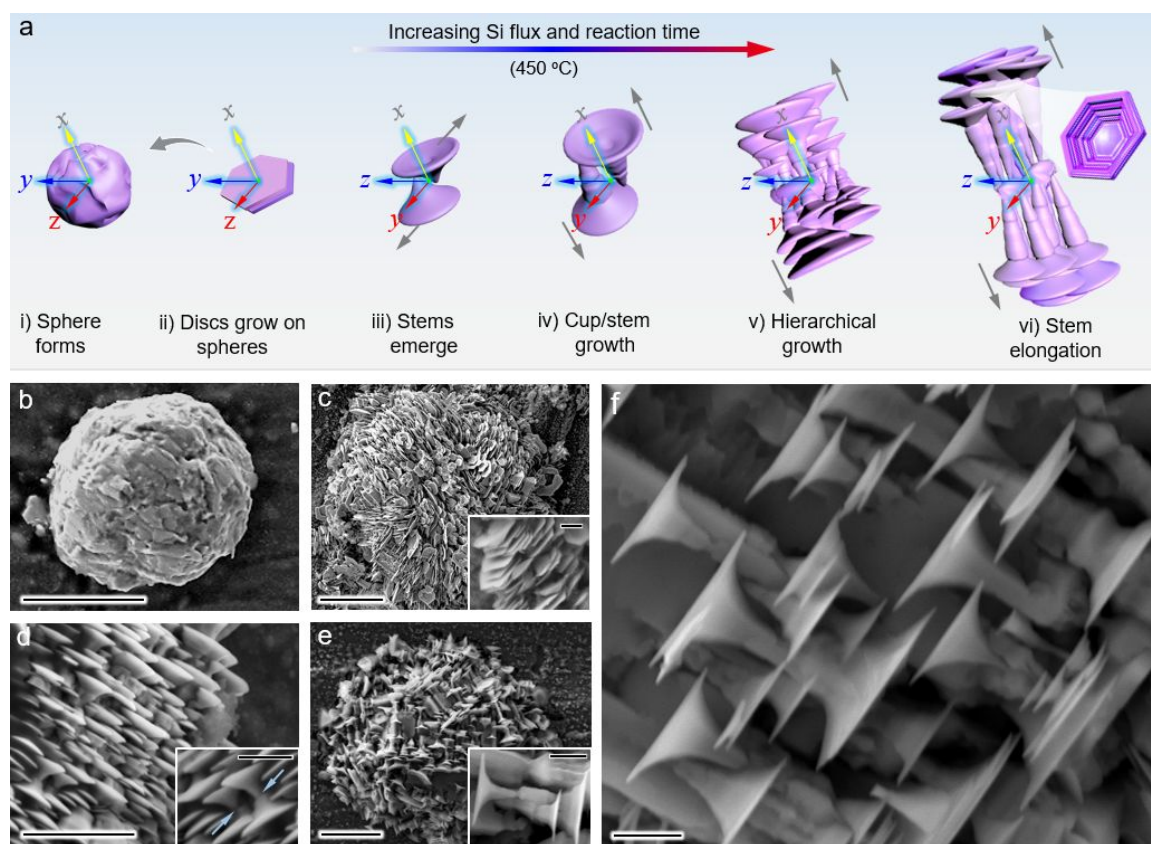


Figure 3 (a) Schematic illustration of the evolution sequence of the $\rho\text{-Cu}_{15}\text{Si}_4$: (i) spherical grains form first, (ii) pair of discs then form on the spherical grains surface, (iii) stems begin to emerge from the inner opposite faces of the discs, (iv) growth of stems and formation of the cup occur, (v) hierarchical growth, and (vi) finally the stems elongate in opposite directions. Gray arrows indicate growth directions along the x -axis, parallel to the growth substrate. SEM images of (b) spherical grains (scale: 10 μm), (c) hexagonal discs clusters grown on the spheres (scale: 10 μm), (d) enlarged image showing the emergence of the stems necking out in opposition directions (scale: 3 μm), and (e, f) cup-stem growth (scale: 10 and 1 μm , respectively).

Growth mechanism of the $\rho\text{-Cu}_{15}\text{Si}_4$. The growth mechanism was qualitatively probed through *ex situ* experimental observations. It is revealed that the $\rho\text{-Cu}_{15}\text{Si}_4$ morphology evolves sequentially through the formation of Cu-rich silicide spheres followed by surface evolution of hexagonal discs, stem growth, and then parallel elongation as illustrated in **Figure 3a**. Typically, interatomic diffusion of Cu and Si atoms triggers *in situ* formation of binary phase Cu-rich silicide spherical grains (**Figure 3b**), about ~ 13.7 μm in average size within ~ 30 min of reaction, which then serve as active sites (silicide islands) to facilitate further crystal growth. Although the Si monomer decomposition is

1
2 expected to occur uniformly on the substrate surface, the formation of the spherical grains is
3
4 spontaneous (non-regulated) as is characteristic of nucleation events. The process of nucleation is
5
6 typically random, with a high potential of occurrence at impurity/defect sites and/or grain
7
8 boundaries,^{36,37} and that may be accountable for the sparse distribution of the spherical grains as
9
10 shown in **Figure S6**. After ~40 min of reaction, the formation of several pairs of hexagonal disc
11
12 clusters on the spherical grains is observed (**Figure 3c**), increasing the overall size (*i.e.* spherical
13
14 grain & discs) to ~31.6 μm .
15
16

17
18 As demonstrated in **Figure S7**, the disc growth possibly evolves through a fluid–solid phase
19
20 transformation mechanism at the interface between Si flux and the spherical grains as Cu inter-
21
22 diffuses with Si atoms.^{27,38} Atomic saturation of the inter-diffused Cu/Si atoms induces coalescence,
23
24 thereby, triggering crystallisation and growth at the crystallite grain surface. Continued reaction with
25
26 flux of Si leads to the gradual emergence of stems, protruding from the inner opposite faces between
27
28 disc pairs as shown in **Figure 3d**. This is facilitated by diffusion of Cu from the Cu-rich crystallite
29
30 spheres to react with Si, as suggested by the slight decrease of overall grain size from ~31.6 to ~22.5
31
32 μm (**Figure S8**). This phenomenon drives a diffusion-induced lateral growth and proliferation of
33
34 interconnected disc-stem features, growing in exactly opposite sides of the growth crystal-base with
35
36 each set seemingly a reflected image of the other (**Figure 3e and f**). Notably, the stems exhibit a
37
38 comparable length as the disc size and a cone-like geometry consistent with the internode features
39
40 observed in Figure 1 and 2.
41
42
43
44
45
46
47

48 **Toward High Density Growth of the $\rho\text{-Cu}_{15}\text{Si}_4$.** An electrochemical process was employed to pre-
49
50 grow discrete Cu crystals on the substrate surface prior to the $\rho\text{-Cu}_{15}\text{Si}_4$ growth. As shown in **Figure**
51
52 **4a** (inset figure), this process leads to the generation of pyramid-like Cu crystals that completely
53
54
55
56
57
58
59
60

cover the Cu-foil surface. As presented in **Figure 4a, b** and **S9**, the conversion of the Cu crystals to Cu-silicide facilitates subsequent growth of high density ρ -Cu₁₅Si₄ with enhanced surface coverage.

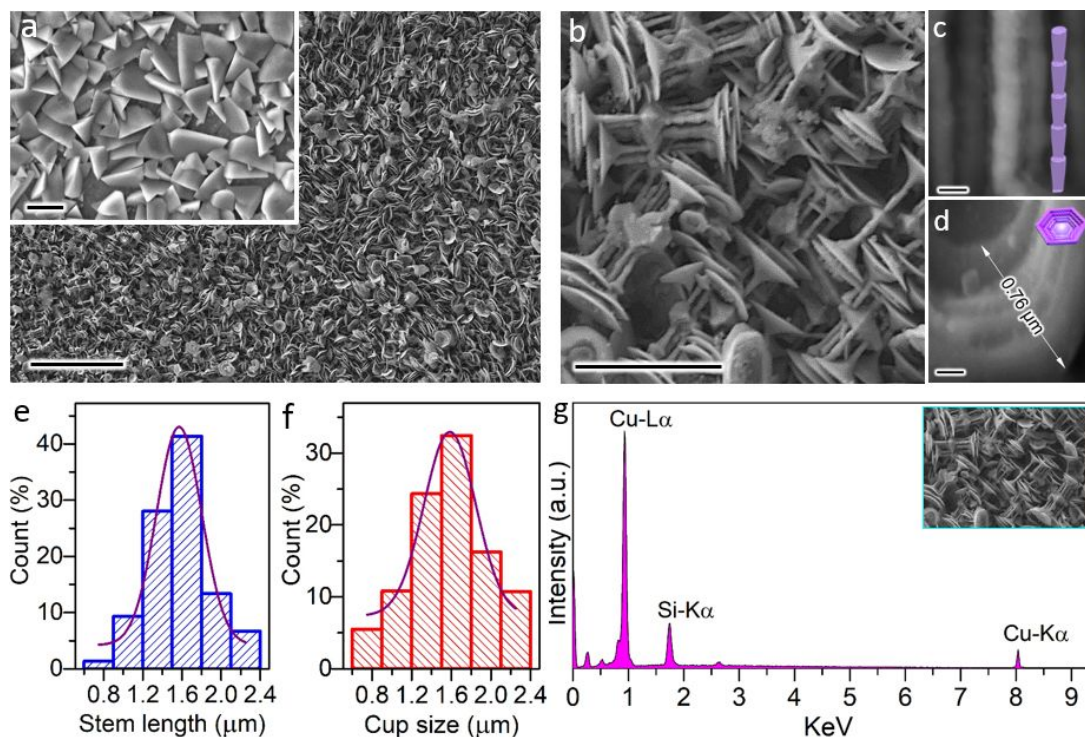


Figure 4 SEM images of (a, b) high density ρ -Cu₁₅Si₄ crystals in high yield at various magnifications (scale: 20 and 5 μ m, respectively). An inset in figure *a* shows the electrochemically pre-grown Cu-crystals (scale: 2 μ m), (c) node-internode feature of the stem (scale: 200 nm), (d) stairs-like layered feature of the cup section (scale: 200 nm), Gaussian-fitted size distribution histogram of the (e) cups (average size: $\sim 1.47 \pm 0.7 \mu$ m) and (f) stems (average size: $\sim 1.58 \pm 0.8 \mu$ m), and (g) EDX spectrum of elemental composition (inset is the corresponding SEM image).

The average stem diameter remains at ~ 150 nm and extends by only $\sim 2.25 \mu$ m in maximum length. However, the average cup size of $\sim 1.47 \mu$ m is relatively higher with a slight distortion of the hexagonal geometry. The occurrence of a relatively shorter stem length could be attributed to lateral growth hindrances, owing to limited growth space for continued elongation. This phenomenon leads to fracture and slight displacement of the grown ρ -Cu₁₅Si₄ with excess reactants resulting in the formation of small particles on the surfaces as seen in **Figure S10**. These observations may be due to

1
2 the high density and random orientations of the pre-grown Cu-crystals that promote high rate silicide
3 growth. Regardless, the stems and cups also exhibit similar node-internode-like features (**Figure 4c**)
4 and layered morphology (**Figure 4d**) with good size distribution as shown in **Figure 4e** and **f** for the
5 cups and stems, respectively. The EDX elemental spectrum (**Figure 4g**) also confirms the presence
6 of both Cu and Si in the ρ -Cu₁₅Si₄ and the growth crystal base (**Figure S11**), indicating that the initial
7 Cu-crystals have also been converted to Cu-silicide during the ρ -Cu₁₅Si₄ growth.
8
9
10
11
12
13
14
15
16
17

18 CONCLUSION

19
20 In summary, we show that a hierarchical ρ -Cu₁₅Si₄ nano-architecture can be laterally grown
21 directly on a Cu-precursor substrate with morphologies consisting of small nanorods, stacked into 1D
22 stems and terminated with concave hexagonally shaped 3D cups. While the stems exhibit node-
23 internode-like features, the cups evolve through a self-regulated layer-by-layer deposition process.
24 The growth mechanism suggests that the interdiffusion of Cu and Si atoms is the strongest driving
25 force for the silicidation process, initially inducing the formation of Cu-rich silicide crystals as active
26 growth islands. The growth orientation is independent of the underlying silicide crystal geometry
27 (spherical or pyramidal) and always grow laterally to the underlying substrate. Electrochemically pre-
28 grown Cu-crystals on the substrate also facilitate direct growth of the ρ -Cu₁₅Si₄ crystals in high yield
29 with enhanced substrate coverage. The results provide new routes and important insights into the
30 growth mechanisms of nanoscale features in transition metal silicides that heretofore were not well
31 understood, and thus, open new avenues to advance the development of TMS at low cost for their
32 wider application in electronic devices.
33
34
35
36
37
38
39
40
41
42
43
44
45
46
47
48
49
50
51
52

53 ASSOCIATED CONTENT

54 Supporting Information

Supporting Information. Details of the experimental section, characterisation methods and supplementary figures. This material is available free of charge via the Internet at:

AUTHOR INFORMATION

Corresponding author: E-mail: kevin.m.ryan@ul.ie, Phone: +353-61 213167

Author Contributions

All authors contributed to the manuscript and have approved of its content and submission.

Notes

The authors declare no competing financial interest.

Acknowledgments

ISA acknowledges funding from the European Union's Horizon 2020 research and innovation programme under the Marie Skłodowska-Curie Individual Fellowship Grant Agreement no: 843621.

KMR acknowledges support by Science Foundation Ireland (SFI) under Grant Number 16/IA/4629 and the SFI Centers, MaREI, AMBER and Confirm, 12/RC/2302_P2, 12/RC/2278_P2 and 16/RC/3918, Irish Research Council (IRC) under Grant Number IRCLA/2017/285. H.G. acknowledges SIRG funding under Grant no. 18/SIRG/5484. M.D.S. and A.H. acknowledge support by the European Research Council (ERC) through a Starting Grant (Agreement no. 716792).

REFERENCES

(1) Schmitt, A. L.; Jin, S. Selective Patterned Growth of Silicide Nanowires without the Use of Metal Catalysts. *Chem. Mater.* **2007**, 19, 126-128.

- 1
2 (2) Schmitt, A. L.; Higgins, J. M.; Szczech, J. R.; Jin, S. Synthesis and Applications of Metal Silicide
3 Nanowires *J. Mater. Chem.* **2010**, *20*, 223-235.
- 4
5
6 (3) Tsai, C.-I.; Yeh, P.-H.; Wang, C.-Y.; Wu, H.-W.; Chen, U.-S.; Lu, M.-Y.; Wu, W.-W.; Chen, L.-
7 J.; Wang, Z.-L. Cobalt Silicide Nanostructures: Synthesis, Electron Transport, and Field Emission
8 Properties. *Cryst. Growth Des.* **2009**, *9*, 4514–4518.
- 9
10
11 (4) Chen, X.; Liang, C. Transition Metal Silicides: Fundamentals, Preparation and Catalytic
12 Applications, *Catal. Sci. Technol.* **2019**, *9*, 4785-4820.
- 13
14
15 (5) Chen, L. J.; Wu, W. W.; Hsu, H. C.; Chen, S. Y.; Chueh, Y. L.; Chou, L. J.; Lu, K. C.; Tu, K. N.
16 Metal Silicide Nanowires. *ECS Trans.* **2007**, *11*, 3–6.
- 17
18
19 (6) Seibt, M.; Griess, M.; Istratov, A. A.; Hedemann, H.; Sattler, A.; Schroter, W. Formation and
20 Properties of Copper Silicide Precipitates in Silicon. *Phys. Status Solidi A* **1998**, *166*, 171–182.
- 21
22
23 (7) Chen, L. J.; Metal Silicides: An Integral Part of Microelectronics, *JOM* **2004**, *57*, 24-30.
- 24
25
26 (8) Buonassisi, T.; Marcus, M. A.; Istratov, A. A.; Heuer, M.; Cizek, T. F.; Lai, B.; Cai, Z.; Weber,
27 E. R. Analysis of Copper-Rich Precipitates in Silicon: Chemical State, Gettering, and Impact on
28 Multicrystalline Silicon Solar Cell Material. *J. Appl. Phys.* **2005**, *97*, 063503-9.
- 29
30
31 (9) Li, C.-P.; Wang, N.; Wong, S.-P.; Lee, C.-S.; Lee, S.-T.; Metal Silicide/Silicon Nanowires from
32 Metal Vapor Vacuum Arc Implantation. *Adv. Mater.* **2002**, *14*, 218–221.
- 33
34
35 (10) Wu, Y.; Xiang, J.; Yang, C.; Lu, W.; Lieber, C. M. Single-Crystal Metallic Nanowires and
36 Metal/Semiconductor Nanowire Heterostructures. *Nature* **2004**, *430*, 61-65.
- 37
38
39 (11) Lin, Y.-C.; Chen, Y.; Huang, Y. The Growth and Applications of Silicides for Nanoscale
40 Devices, *Nanoscale* **2012**, *4*, 1412-1421.
- 41
42
43 (12) Chueh, Y.-L.; Ko, M.-T.; Chou, L.-J.; Chen, L.-J.; Wu, C.-S.; Chen, C.-D. TaSi₂ Nanowires: A
44 Potential Field Emitter and Interconnect. *Nano Lett.* **2006**, *6*, 1637–1644.
- 45
46
47
48
49
50
51
52
53
54
55
56
57
58
59
60

- 1
2 (13) Szczech, J. R.; Schmitt, A. L.; Bierman, M. J.; Jin, S. Single-Crystal Semiconducting Chromium
3 Disilicide Nanowires Synthesized via Chemical Vapor Transport. *Chem. Mater.* **2007**, *19*, 13, 3238–
4 3243.
5
6
7
8 (14) Geaney, H.; Dickinson, C.; O' Dwyer, C.; Mullane, E.; Singh, A.; Ryan, K. M. Growth of
9 Crystalline Copper Silicide Nanowires in High Yield within a High Boiling Point Solvent System.
10
11 *Chem. Mater.* **2012**, *24*, 4319–4325.
12
13 (15) Sheehan, M.; Ramasse, Q. M.; Geaney, H.; Ryan, K. M. Linear Heterostructured Ni₂Si/Si
14 Nanowires with Abrupt Interfaces Synthesised in Solution. *Nanoscale* **2018**, *10*, 19182-19187.
15
16 (16) Hou, Q. R.; Gu, B. F.; Chen, Y. B.; He, Y. J.; Sun, J. L. Layer-by-layer Deposition of MnSi_{1.7}
17 Film with high Seebeck Coefficient and Low Electrical Resistivity. *Mater. Chem. Phys.* **2014**, *146*,
18 346-353.
19
20 (17) Zhou, F.; Szczech, J.; Pettes, M. T.; Moore, A. L.; Jin, S.; Shi, L. Determination of Transport
21 Properties in Chromium Disilicide Nanowires via Combined Thermoelectric and Structural
22 Characterizations. *Nano Lett.* **2007**, *7*, 1649–1654.
23
24 (18) Giannini, C.; Lagomarsino, S.; Scarinci, F.; Castrucci, P. Nature of the Band Gap of
25 Polycrystalline *p*-FeSi₂ Films. *Phys. Rev. B*, **1992**, *45*, 8822–8824.
26
27 (19) Ahmed, S. J.; Boyer, C.; Niewczas, M. Magnetic and Structural Properties of Co₂MnSi based
28 Heusler Compound. *J. Alloys Comp.* **2019**, *781*, 216–225.
29
30 (20) Hsu, H.-F.; Chen, C.-A.; Liu, S.-W.; Tang, C.-K. Fabrication and Gas-Sensing Properties of Ni-
31 Silicide/Si Nanowires. *Nanoscale Res. Lett.* **2017**, *12*, 1–8.
32
33 (21) Lin, Y.-C.; Lu, K.-C.; Wu, W.-W.; Bai, J.; Chen, L. J.; Tu, K. N.; Huang, Y. Single Crystalline
34 PtSi Nanowires, PtSi/Si/PtSi Nanowire Heterostructures and Nanodevices. *Nano Lett.*, **2008**, *8*, 913–
35 918.
36
37
38
39
40
41
42
43
44
45
46
47
48
49
50
51
52
53
54
55
56
57
58
59
60

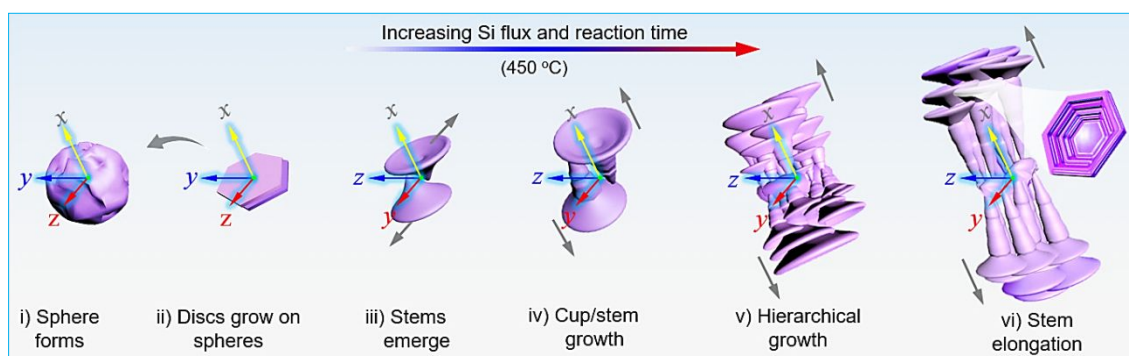
- 1
2 (22) Johnson, D. C.; Mosby, J. M.; Riha, S. C. Prieto, A. L. Synthesis of Copper Silicide
3 Nanocrystallites Embedded in Silicon Nanowires for Enhanced Transport Properties. *J. Mater. Chem.*
4 **2010**, *20*, 1993–1998.
5
6
7
8 (23) Stokes, K.; Geaney, H.; Sheehan, M.; Borsa, D.; Ryan, K. M. Copper Silicide Nanowires as
9 Hosts for Amorphous Si Deposition as a Route to Produce High Capacity Lithium-Ion Battery
10 Anodes. *Nano Lett.* **2019**, *19*, 8829–8835.
11
12
13 (24) Hymes, S.; Kumar, K. S.; Murarka, S. P.; Ding, P. J.; Wang, W.; Lanford, W. A. J.; Thermal
14 Stability of Copper Silicide Passivation Layers in Copper-Based Multilevel Interconnects. *Appl.*
15 *Phys.* **1998**, *83*, 4507–4512.
16
17 (25) Aminu, I. S.; Geaney, H.; Imtiaz, S.; Adegoke, T. E.; Kapuria, N.; Collins, G. A.; Ryan, K. M.
18 A Copper Silicide Nanofoam Current Collector for Directly Grown Si Nanowire Networks and their
19 Application as Lithium-Ion Anodes. *Adv. Funct. Mater.* **2020**, 2003278.
20
21 (26) Sufryd, K.; Ponweiser, N.; Riani, P.; Richter, K. W.; Cacciamani, G. Experimental Investigation
22 of the Cu-Si Phase Diagram at $x(\text{Cu}) > 0.72$. *Intermetallics* **2011**, *19*, 1479–1488.
23
24 (27) Jung, S.J.; Lutz, T.; Bell, A. P.; McCarthy, E. K.; Boland, J. J. Free-Standing, Single-Crystal
25 Cu_3Si Nanowires. *Cryst. Growth Des.* **2012**, *12*, 3076–3081.
26
27 (28) Jung, S.J.; O' Kelly, C. J.; Boland, J. J. Position Controlled Growth of Single Crystal Cu_3Si
28 Nanostructures. *Cryst. Growth Des.* **2015**, *15*, 5355–5359.
29
30 (29) Li, S.; Cai, H.; Gan, C. L.; Guo, J.; Dong, Z.; Ma, J. Controlled Synthesis of Copper-Silicide
31 Nanostructures. *Cryst. Growth Des.* **2010**, *10*, 2983–2989.
32
33 (30) Zhang, Z.; Wong, L.M.; Ong, H.G.; Wang, X.J.; Wang, J. L.; Wang, S. J.; Chen, H.; Wu, T. Self-
34 Assembled Shape- and Orientation-Controlled Synthesis of Nanoscale Cu_3Si Triangles, Squares, and
35 Wires. *Nano Lett.* **2008**, *8*, 3205–3210.
36
37
38
39
40
41
42
43
44
45
46
47
48
49
50
51
52
53
54
55
56
57
58
59
60

- 1
2 (31)Kukushkin, S. A.; Osipov, A. V. First-Order Phase Transition through an Intermediate State.
3
4 *Phys. Solid State*, **2014**, *56*, 792–800.
5
6 (32)Kukushkin, S. A.; Sakalo, T. V. Diffusional Coalescence of Island Films on the Real Crystal
7
8 Surface in the Case of Layer-by-Layer Growth of Islands–I. An Isolated System. *Acta Metal. Mater.*,
9
10 **1993**, *41*, 1237–1241.
11
12 (33)Kukushkin, S. A.; Sakalo, T. V. Diffusional Coalescence of Island Films on the Real Crystal
13
14 Surface in the Case of Layer-by-Layer Growth of Islands–II. An Open System. Undamped Sources
15
16 of Deposited Atoms. *Acta Metal. Mater.*, **1993**, *41*, 1243–1244.
17
18 (34)Sakalo, T. V.; Kukushkin, S. A. Diffusional Coalescence of Island Films on the Real Crystal
19
20 Surface in the Case of Layer-by-Layer Growth of Islands–IV. Theory and Experiment. *Acta Metal.*
21
22 *Mater.*, **1994**, *42*, 2803–2810.
23
24 (35)Chromik, R. R.; Neils, W. K.; Cotts, E. J. Thermodynamic and kinetic study of Solid State
25
26 Reactions in the Cu–Si System. *J. Appl. Phys.* **1999**, *86*, 4273–4281.
27
28 (36)Yizhi, Z.; Senbo, X.; Verner, H.; Jianying, H.; Zhiliang, Z.; Anti-icing Ionogel Surfaces:
29
30 Inhibiting Ice Nucleation, Growth, and Adhesion, *ACS Materials Lett.* **2020**, *2*, 616–623.
31
32 (37)P. D. Kanungo, R. Koegler, N. Zakharov, P. Werner, R. Scholz, W. Skorupa, Characterization
33
34 of Structural Changes Associated with Doping Silicon Nanowires by Ion Implantation. *Cryst. Growth*
35
36 *Des.* 2011, **11**, 2690 –2694.
37
38 (38)Li, J.; Wang, Z.; Deepak, F. L. In Situ Atomic-Scale Observation of Droplet Coalescence Driven
39
40 Nucleation and Growth at Liquid/Solid Interfaces. *ACS Nano* **2017**, *11*, 5590 –5597.
41
42
43
44
45
46
47
48
49
50
51
52
53
54
55
56
57
58
59
60

For Table of Contents Use Only**Evolution of Hierarchically-Layered Cu-rich Silicide Nano-Architectures**

Ibrahim Saana Amiin, Nilotpal Kapuria, Temilade Esther Adegoke, Angelika Holzinger,

Hugh Geaney, Micheál D. Scanlon, Kevin M. Ryan*

**Synopsis**

A Cu-rich silicide nano-architecture (ρ -Cu₁₅Si₄), consisting of a stack of nanorods (~300 nm in length) and terminated with concave hexagonal 3D cups that evolves through a self-regulated layer-by-layer growth mechanism is demonstrated. The structural evolution is governed by interatomic diffusion, initially triggering the formation of binary-phase silicide islands (spheres) followed by the formation of hexagonal discs, stem growth, and lateral elongation in exactly opposite directions.